NASA TECHNICAL NOTE

NASA TN D-2610

NASA TN D-2610

LAMINAR BOUNDARY-LAYER SEPARATION INDUCED BY FLARES ON CYLINDERS WITH HIGHLY COOLED BOUNDARY LAYERS AT A MACH NUMBER OF 15

by Donald M. Kuehn

Ames Research Center
Moffett Field, Calif.

NATIONAL AERONAUTICS AND SPACE ADMINISTRATION • WASHINGTON, D. C. • JANUARY 1965

LAMINAR BOUNDARY-LAYER SEPARATION INDUCED BY FLARES ON CYLINDERS WITH HIGHLY COOLED BOUNDARY LAYERS AT A MACH NUMBER OF 15

By Donald M. Kuehn

Ames Research Center
Moffett Field, Calif.

NATIONAL AERONAUTICS AND SPACE ADMINISTRATION

For sale by the Office of Technical Services, Department of Commerce,
Washington, D.C. 20230 -- Price $2.00

LAMINAR BOUNDARY-LAYER SEPARATION INDUCED BY FLARES ON CYLINDERS WITH HIGHLY COOLED BOUNDARY LAYERS AT A MACH NUMBER OF 15

By Donald M. Kuehn

Ames Research Center
Moffett Field, Calif.

SUMMARY

Incipient separation of a laminar boundary layer was experimentally investigated on a blunted cylinder-flare configuration at zero angle of attack. Conical flares with various angles were tested with each of three nose shapes in air at a nominal Mach number of 15. The nose shapes included a spherical-tipped cone, a hemisphere, and a flat face. Equilibrium stagnation temperature was about 3600° R, and the surface temperature of the models was about 550° R; thus the boundary layers on all models were highly cooled. The Reynolds numbers, based on free-stream properties for equilibrium flow and on cylinder diameter, were about 2400 and 6200. Incipient separation was believed to occur at a flare angle between 35° and 40° for all three nose shapes. A comparison of the present data with previously published data showed that the very low Reynolds number and substantial boundary-layer cooling of the present tests were highly favorable for maintaining an attached boundary layer for very large flow-deflection angles.

INTRODUCTION

Gasdynamic properties at the surface must be known in order to predict the flight characteristics of a vehicle. In many cases these properties are altered sufficiently by the occurrence of boundary-layer separation so that it is necessary to know whether the boundary layer will be attached or separated. Existing theories do not successfully predict the flow conditions and body geometries for which separation can be expected. Experimental data that can be used to predict separation have therefore been obtained (e.g., refs. 1 and 2); however, more experiments are required for body shapes and test conditions for which there are no data.

The purpose of the present experimental investigation is to contribute to the knowledge of incipient, laminar boundary-layer separation. The test conditions of the experiments on cylinder-flare configurations reported in reference 2 were extended in the present tests to a lower Reynolds number, to a higher free-stream Mach number, and to a significant amount of boundary-layer cooling. These test conditions approximately correspond to full-scale flight at a Mach number of 15 and an altitude between 200,000 and 300,000 feet.

The occurrence of separation was estimated from measurements of surface pressures on models with and without flares. In order to facilitate comparison of present and previous data and to permit application of the data to cases other than those tested, approximate calculations were made of the inviscid-viscid attached flow about the models without the flares.

NOTATION

D	cylinder diameter, in.
h	enthalpy, Btu/lb
l	distance from the tip of the model nose to the beginning of the flare, in.
M	Mach number
p	pressure, psia
p_x	pressure on the cylinder at station x
r	radial distance measured from the longitudinal axis of the cylinder, in.
R	Reynolds number
T	temperature, ^{o}R
x	distance along the cylinder axis measured from the tip of the nose, or distance from the leading edge of a flat plate, in.
x_o	the approximate value of x to the farthest upstream influence of the flare on the surface pressures, in.
θ	half-angle of the conical flare, deg
δ	boundary-layer thickness, in.

Subscripts

D,x,δ	reference dimensions for Reynolds number
e	boundary-layer edge
n	nose of the model

t	total conditions
w	wall of the model
∞	free stream
incip	condition for incipient separation
1	upstream of the normal shock wave

TEST CONDITIONS, MODELS, AND MEASUREMENTS

The test conditions and the instrumentation were the same as were used in the experiments reported in reference 3. The blunt cylinders were also the same except for flares which were added for the present tests. Appropriate discussion in reference 3 is, therefore, applicable to the present report. To avoid unnecessary duplication only selected pertinent information will be repeated here. (Details of the test apparatus and the determination and description of flow properties can be found in ref. 3.)

Test Conditions

The models were tested in an arc-heated air stream. A nominal Mach number of 15 was attained with a conical nozzle of 15° half-angle. Gradients of Mach number and pressure along the nozzle center line due to the conical flow are shown in reference 3. Total enthalpy was about 1000 Btu/lb; nozzle reservoir pressures were about 380 and 1000 psia. Reynolds numbers, based on equilibrium stream properties and on cylinder diameter, were about 2400 and 6200. The presence of nonequilibrium flow in the test nozzle and over the models was considered in reference 3. The amount of energy involved in the nonequilibrium process was so small that the flow can be considered to be in equilibrium.

Models

The models were blunt, stream-alined cylinders with conical flares. The geometry of the models is shown in figure 1. During the test period the base diameter of the 35° flare was decreased to prevent tunnel blockage. Consequently, the shape of this flare differed from the others. A single static pressure orifice was located in one section of the cylinder. To obtain pressures at other stations cylindrical extensions were inserted between the nose and that section which contained the orifice. The location of the nose was maintained at the same tunnel station for all cylindrical extensions. The longitudinal position of the flare on the cylinder was

adjusted to maintain the cylinder length shown in figure 1. The distance from the tip of the nose to the flare was not the same for all models because of the slightly different nose lengths.

Measurements

Measurements of cylinder-surface pressures and photographs of the shock-wave patterns were obtained. Pressure transducers (see ref. 3) were used and the output of each transducer was measured with an Offner recorder. The duration of a typical run was about 4 seconds which, from the work of reference 3, allowed sufficient time to overcome the lag in the pressure-measuring system. Copper tubing was used throughout the pressure-measuring system, except where short sections of plastic connectors were necessary. The system was thoroughly evacuated for several days before any measurements were made. The shock waves about the models were observed by the use of the glow-discharge technique (described briefly in ref. 3). Selected photographs are shown in figure 2. The portion of the flare-induced shock wave that was visible in each of the original photographs was traced with dashed lines in the bottom half of the photograph.

RESULTS AND DISCUSSION

Attached Flow About the Blunt Cylinders

In this study of flare-induced boundary-layer separation, a description was needed of the local inviscid-flow properties and the attached boundary layer so that the present data on incipient separation would be useful in the prediction of separation on other vehicles having similar local-flow properties. The local-flow properties considered to be the most important to separation are Mach number, boundary-layer-edge Reynolds number, and the amount of boundary-layer cooling (e.g., see refs. 1 and 2). The inviscid flow over the present blunt cylinders is characterized by large variations in local Mach number and Reynolds number along, and normal to, the streamlines. A thick laminar boundary layer is probable for the low Reynolds number of the present tests. This boundary layer will extend far into the nonuniform flow field and will therefore be subjected to a wide range of local-flow properties. This, of course, complicates the boundary-layer thickness calculations. An accurate analysis of the viscid-inviscid flow for these circumstances was beyond the scope of the present investigation. Therefore, an approximate analysis was made. The air in the test nozzle and over the model was assumed to be in equilibrium. (The difference between frozen and equilibrium values of Mach number and Reynolds number at the wall for inviscid flow are less than 10 percent and 20 percent, respectively. These differences were probably not significant to the estimated boundary layer, or to incipient separation.) Flat-plate theory was used in estimating the boundary layer on the cylinder and any interaction between the viscid and inviscid flow was neglected.

The properties of inviscid, equilibrium air flow around the blunt cylinders were estimated at several longitudinal stations by means of the continuity method of reference 4 which is shown in reference 5 to give a fair description of the over-all flow field. Mach numbers and unit Reynolds numbers determined by these inviscid-flow calculations are shown in figure 3.

Van Driest's flat-plate theory (ref. 6) was used to estimate the thickness of the laminar boundary layer for each of the blunt cylinders (an estimate discussed in the following paragraph indicated that the boundary layer probably was laminar). Simplicity was the primary justification for using flat-plate theory; however, a limited comparison (fig. 4) of the boundary-layer thickness from flat-plate theory with experimental values from the investigations reported in references 2 and 7 indicated that this estimate might be suitable, at least for thin boundary layers. The applicability of this flat-plate estimation is unknown for thick axisymmetric boundary layers at high free-stream Mach numbers where there is a significant variation of flow properties through, as well as along, the boundary layer (the estimated value of boundary-layer thickness on the present cylinders will be shown later to be ~0.6D). It is not clear, therefore, how to choose the value of flat-plate Reynolds number that will give a boundary-layer thickness equal to that of an axisymmetric boundary layer in the environment just described. Lacking this insight, the thicknesses of flat-plate boundary layers were determined in the present analysis for the two values of edge unit Reynolds numbers believed to represent the approximate extremes that could affect the growth of the boundary layer; one value represented the minimum Reynolds number at the boundary-layer edge (farthest downstream) and the other represented the maximum edge Reynolds number (farthest upstream). For a first approximation, wall Reynolds number determined at the station at which the flare will begin (fig. 3) was used to compute a flat-plate boundary layer. The inviscid flow field was then examined to establish the minimum Reynolds number along the edge of the boundary layer. This minimum Reynolds number was then used to recompute the boundary layer. The procedure was repeated until the minimum edge Reynolds number agreed approximately with the value used in the calculation. The thickness of this boundary layer was believed to be the approximate maximum. The approximate minimum was determined from values of maximum Reynolds number along the boundary-layer edge. The actual boundary layer probably develops according to some integrated value of Reynolds number along the boundary layer that will likely be between the minimum and maximum values just described. These values of boundary-layer thickness (fig. 3) were used as the reference dimensions for Reynolds number.

Length Reynolds number based on properties at the edge of the estimated boundary layer indicated that the boundary layer was laminar. An approximate upper limit of the length Reynolds number to the beginning of the flare, based on the maximum value of R_e/inch (fig. 3), was about 10^4. The length Reynolds number based upon an integrated value of R_e/inch along the boundary layer could be considerably less than 10^4, however, because R_e/inch decreases very rapidly downstream along the boundary-layer edge. Since the minimum transition Reynolds number is probably of the order of 10^6, transition appears to have been downstream of the region of interest by a safe margin.

Another indication of the boundary-layer thickness can be deduced from the flare-induced shock wave in the glow-discharge photographs. Generally, a laminar boundary layer fills in (or effectively rounds) a sharp corner so that the external flow is turned gradually. For thin boundary layers, this gradual turning generates weak waves (not apparent in visual-flow photographs) that coalesce into a strong, visible shock outside of the boundary layer (e.g., see ref. 2). If the coalesced shock wave always appears outside of the laminar boundary layer for thicker boundary layers also, an upper limit to the boundary-layer thickness on the present models might be indicated by the distance from the body surface to the first appearance of this shock in the photographs of figure 2. (Reproduction of low contrast photographs loses details that were apparent in the originals, so shock waves that were visible in the original photographs were traced with dashed lines in the lower half of the photographs.) By this criterion, the photographs of the models with attached flow ($\theta \lesssim 35^\circ$) indicate that the boundary layer in the region of the cylinder-flare juncture was, in general, no thicker than about one half the shock-layer thickness. This upper limit is consistent with the rough theoretical estimate.

Incipient Boundary-Layer Separation

Surface pressure distributions were used to detect the occurrence of boundary-layer separation. These pressure distributions on cylinders with flares (present measurements) and without flares (ref. 3) are shown in figures 5 to 7. The measured pressures were not corrected for the nozzle-stream gradient since the corrections would not affect the comparison between the pressure distributions with and without a flare.

The occurrence of flare-induced boundary-layer separation was judged by examining the upstream influence of the flare on the cylinder surface pressures. This upstream influence, obtained from figures 5 to 7, is shown in figure 8 as a function of flare angle for each nose shape. Experience obtained in previous investigations of boundary-layer separation (e.g., refs. 1 and 2) showed that the upstream influence of a compression corner on surface pressure is smaller and less sensitive to changes in corner angle for an attached boundary layer than for a separated boundary layer. On this basis, the abrupt change in the upstream influence that occurred as the flare angle on the conical-nosed model was increased from 35° to 40° (see fig. 8) was interpreted to be indicative of the occurrence of significant separation. (The possibility that a detached shock at the flare was responsible for the abrupt change in the upstream influence is believed to be unlikely, as discussed in the following paragraph.) The hemispherical- and flat-nosed models were not tested with a sufficient number of flare angles to determine the angle at which the upstream influence changed abruptly. It is believed, however, that the rate of change of upstream influence with flare angle should be about the same for all nose shapes. This belief is supported by references 1 and 2 which show that flare-induced separation on cylinders with different nose

shapes is qualitatively similar. The conclusion is, therefore, that the first occurrence of separation appears to take place at a flare angle between 35° and 40° for all three nose shapes.

Although the largest flare angle used in the present investigation slightly exceeded the two-dimensional shock-detachment angle, it is not probable that shock detachment caused the abrupt change in upstream influence. A two-dimensional shock-detachment angle would apply to inviscid flow; however, the presence of a boundary layer will cause a significant departure from two-dimensional flow. Reference 1 contains evidence that viscous flow in the region of a cylinder-flare juncture is not two-dimensional and gives several examples where the flare angle has exceeded the two-dimensional detachment angle with no apparent evidence of shock detachment. The magnitude of departure from two-dimensional flow can be estimated by computing the theoretical values of pressure rise for two-dimensional and conical flow and comparing these values with the experimental pressure distributions of reference 1. This comparison shows that the maximum pressure rise on the flare, which occurs near the corner, was lower than the two-dimensional value by about 70 to 80 percent of the difference between the two-dimensional and conical values. Therefore, the shock-detachment angle is probably much closer to the conical than to the two-dimensional value. The boundary layers in the present experiments were much thicker than those of reference 1; thus the departure from two-dimensional flow in the present experiments should be even greater than that of reference 1. Using the minimum value of inviscid Mach number near the beginning of the flare for the blunt conical-nosed model of the present investigation will give a shock detachment angle for two-dimensional flow of about 37° and for conical flow about 52°. From the above discussion, it appears that the detachment angle for the present flares should be well above the maximum flare angle tested. Further evidence that shock detachment did not occur is indicated by the Reynolds number effect on the extent of boundary-layer separation shown in figures 5(e) and 5(f). Shock detachment is not likely to be so sensitive to Reynolds number variation, whereas the Reynolds number effect shown in this figure is consistent with previous investigations for a separated boundary layer not influenced by shock detachment (e.g., refs. 1 and 2).

Previous investigations have shown that Reynolds number and boundary-layer cooling are important to separation, but more data are required so that the quantitative effects of these two variables can be determined over a wider range of test conditions. The present data provide some information on these two variables at a very low Reynolds number; however, the individual effects of Reynolds number and boundary-layer cooling cannot be distinguished. Existing data show that the tendency toward separation is reduced as Reynolds number is decreased for an adiabatic wall, or as boundary-layer cooling is increased at a constant Reynolds number (e.g., refs. 2, 8, 9, 10). Even for the small Reynolds number range covered in the present tests, Reynolds number continues to be important for highly cooled walls (cf. figs. 5(e) and 5(f)). This effect of Reynolds number is qualitatively the same as shown by the data for adiabatic walls (ref. 2). The combined effect of low Reynolds number plus substantial boundary-layer cooling on the flare angle for incipient separation can be seen in figure 9 where the present data are compared with

that of reference 2. Only one data point is shown for the present data because the estimates of local-flow properties for the present models were not sufficiently accurate to differentiate between the different models. Thus a range of conditions is shown by the bars and includes the estimates for all models.

CONCLUDING REMARKS

Comparison of the present and existing experiments showed that the maximum angle through which the laminar boundary layer would turn and remain attached was considerably increased by the combined influence of very low Reynolds number plus substantial boundary-layer cooling. In these experiments, the boundary layer turned through an angle greater than 35° without separating from the surface, whereas previous data for uncooled, laminar boundary layers at higher Reynolds numbers showed the turning angle to be about 10° or less.

Ames Research Center
National Aeronautics and Space Administration
Moffett Field, Calif., Oct. 23, 1964

REFERENCES

1. Kuehn, Donald M.: Turbulent Boundary-Layer Separation Induced by Flares on Cylinders at Zero Angle of Attack. NASA TR R-117, 1961.

2. Kuehn, Donald M.: Laminar Boundary-Layer Separation Induced by Flares on Cylinders at Zero Angle of Attack. NASA TR R-146, 1962.

3. Kuehn, Donald M.: Experimental and Theoretical Pressures on Blunt Cylinders for Equilibrium and Nonequilibrium Air at Hypersonic Speeds. NASA TN D-1979, 1963.

4. Seiff, Alvin, and Whiting, Ellis E.: Calculation of Flow Fields From Bow-Wave Profiles for the Downstream Region of Blunt-Nosed Circular Cylinders in Axial Hypersonic Flight. NASA TN D-1147, 1961.

5. Terry, James E., and James, Carlton S.: A Parametric Study of Hypersonic Flow Fields About Blunt-Nosed Cylinders at Zero Angle of Attack. NASA TN D-2342, 1964.

6. Van Driest, E. R.: Investigation of Laminar Boundary Layer in Compressible Fluids Using the Crocco Method. NACA TN 2597, 1952.

7. Kubota, Toshi: Investigation of Flow Around Simple Bodies in Hypersonic Flow. GALCIT Memo. 40, 1957.

8. Curle, N.: The Effects of Heat Transfer on Laminar Boundary Layer Separation in Supersonic Flow. British ARC 21,986 - F. M. 2965, 1960.

9. Gadd, G. E., and Attridge, J. L.: A Note on the Effects of Heat Transfer on the Separation of a Laminar Boundary Layer. British ARC 22,558 - F. M. 3050, 1961.

10. Lankford, J. L.: The Effect of Heat Transfer on the Separation of Laminar Flow Over Axisymmetric Compression Surfaces. Preliminary Results at Mach Number 6.78. NAVWEP Rep. 7402, 1961.

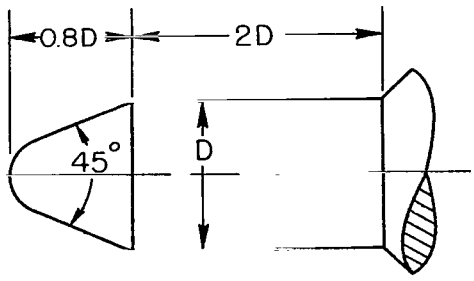

Blunt conical nose (diameter of the spherical tip on the cone = D/2)

D = 0.625 inch

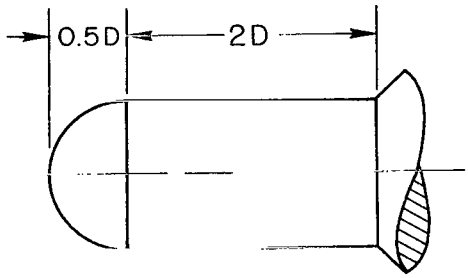

Hemispherical nose

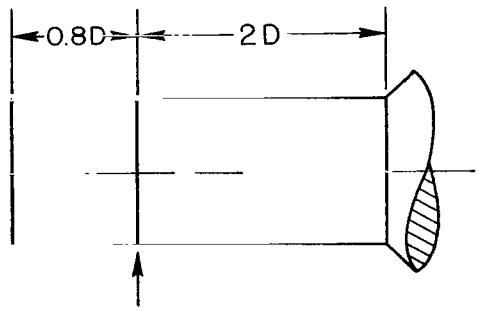

Flat nose

Juncture between the removable nose and the cylinder

(a) Nose cylinder.

Figure 1.- Test models.

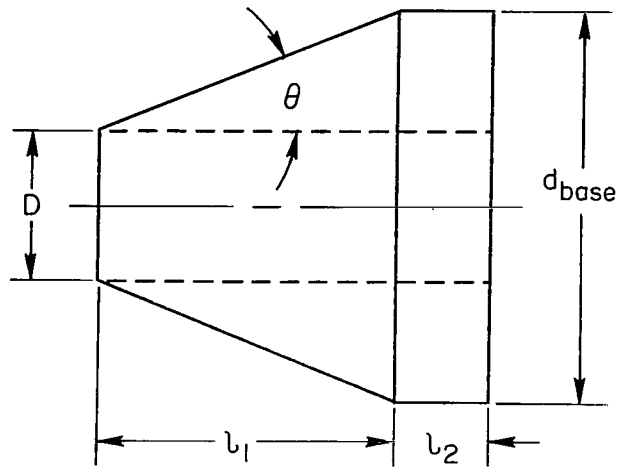

D = 0.625 inch

θ, deg	$\frac{l_1}{D}$	$\frac{l_2}{D}$	$\frac{d_{base}}{D}$
15	2.50	0	2.34
25	2.50	0	3.33
30	2.00	0	3.31
35	1.35	0.24	2.89
40	1.00	0	2.68

(b) Flares.

Figure 1.- Concluded.

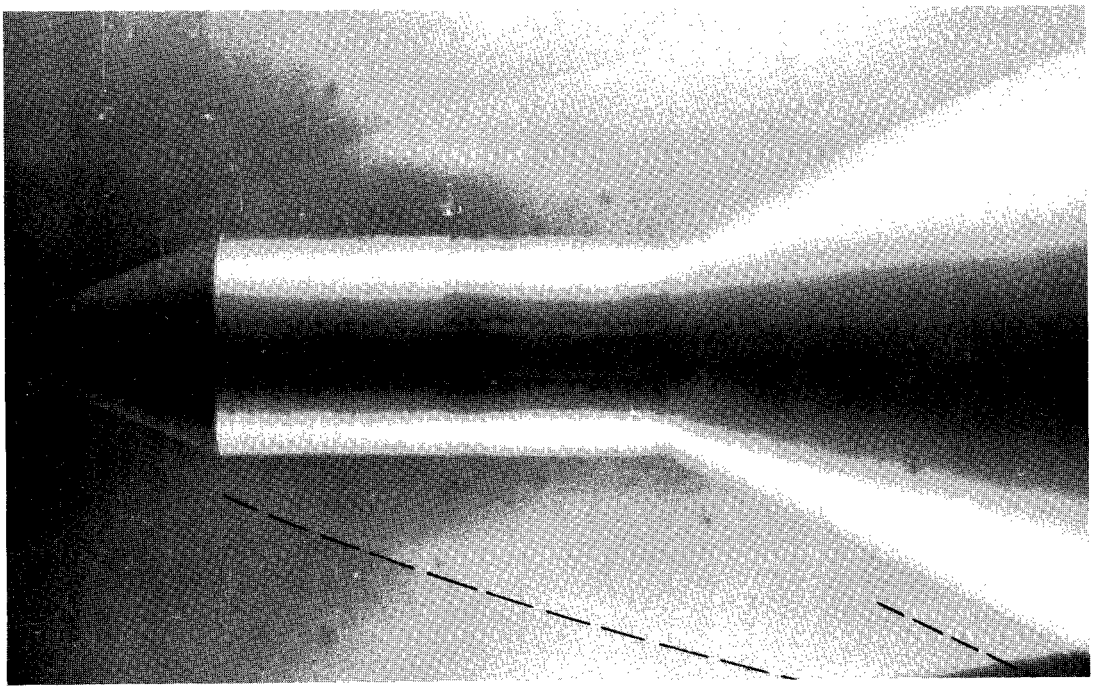

(a) Blunt conical nose; $\theta = 25^{\circ}$.

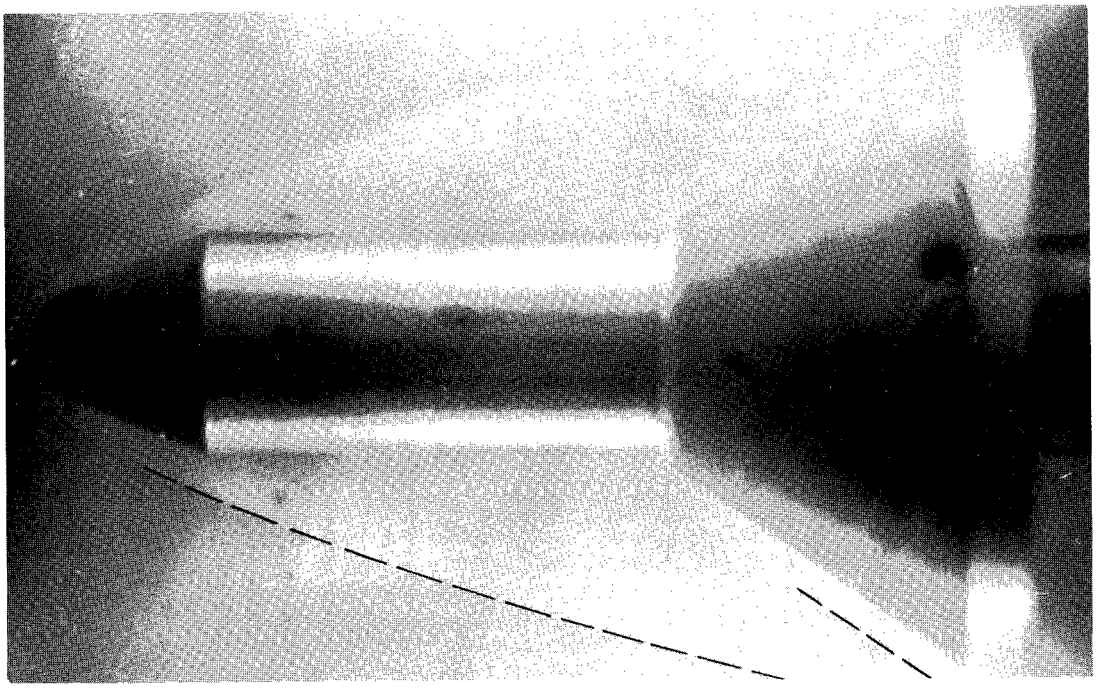

(b) Blunt conical nose; $\theta = 35^{\circ}$.

Figure 2.- Typical photographs of the flow field using the glow-discharge technique.

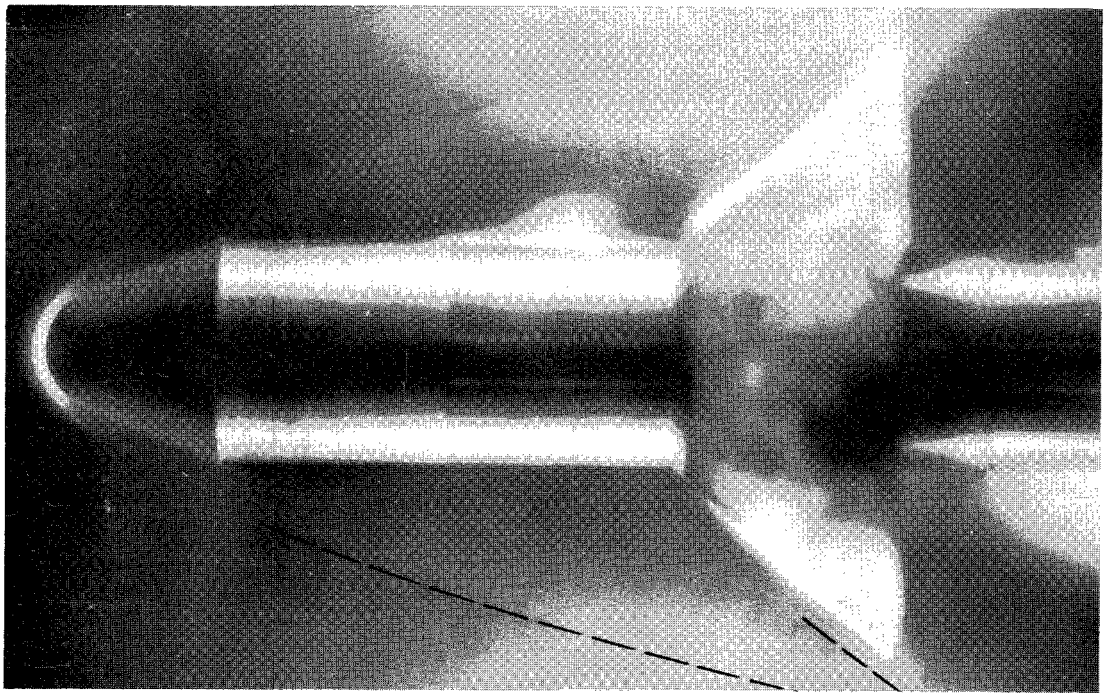

(c) Blunt conical nose; $\theta = 40^{\circ}$.

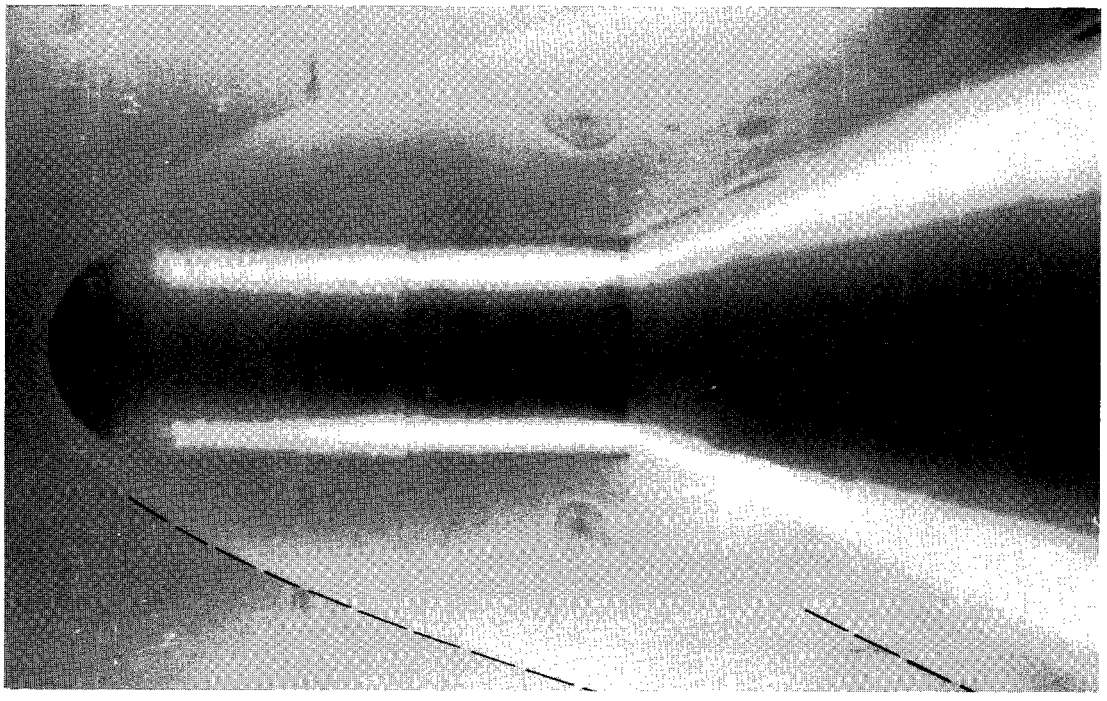

(d) Hemispherical nose; $\theta = 25^{\circ}$.

Figure 2.- Continued.

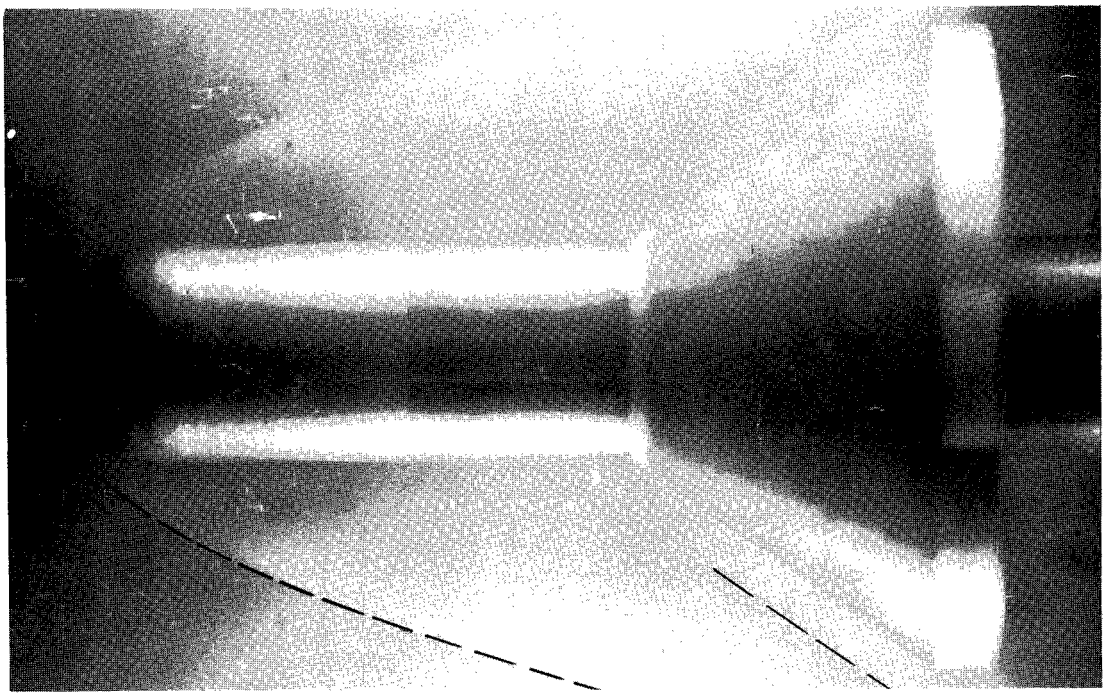

(e) Hemispherical nose; $\theta = 35^{\circ}$.

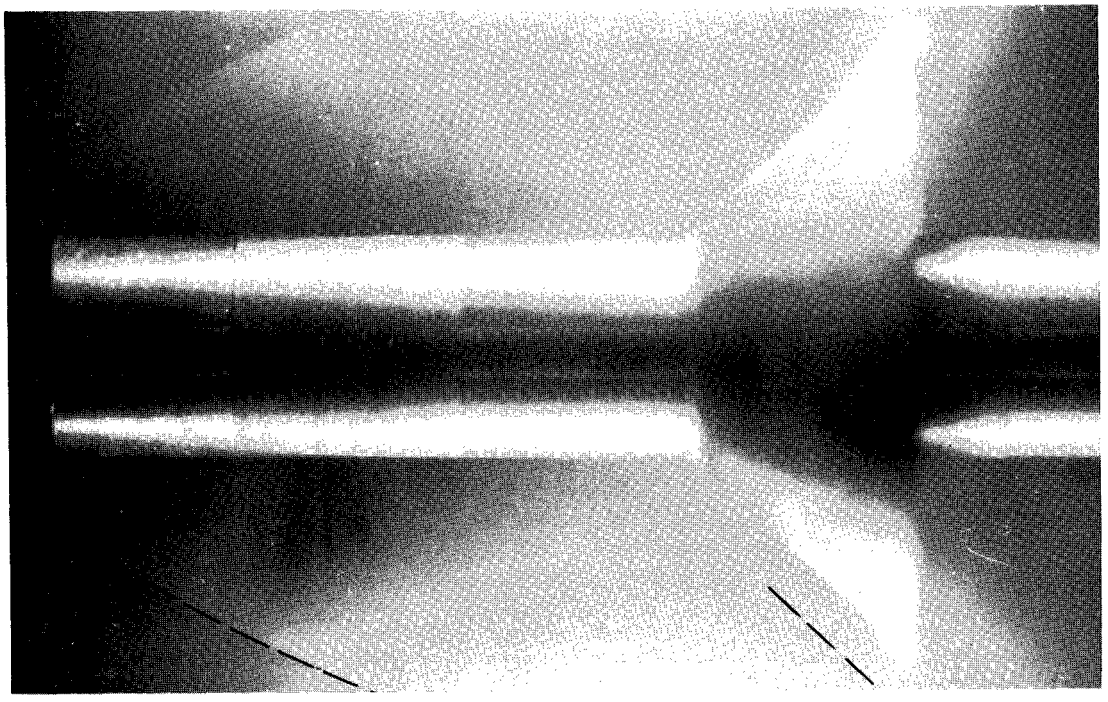

(f) Flat nose; $\theta = 40^{\circ}$.

Figure 2.- Concluded.

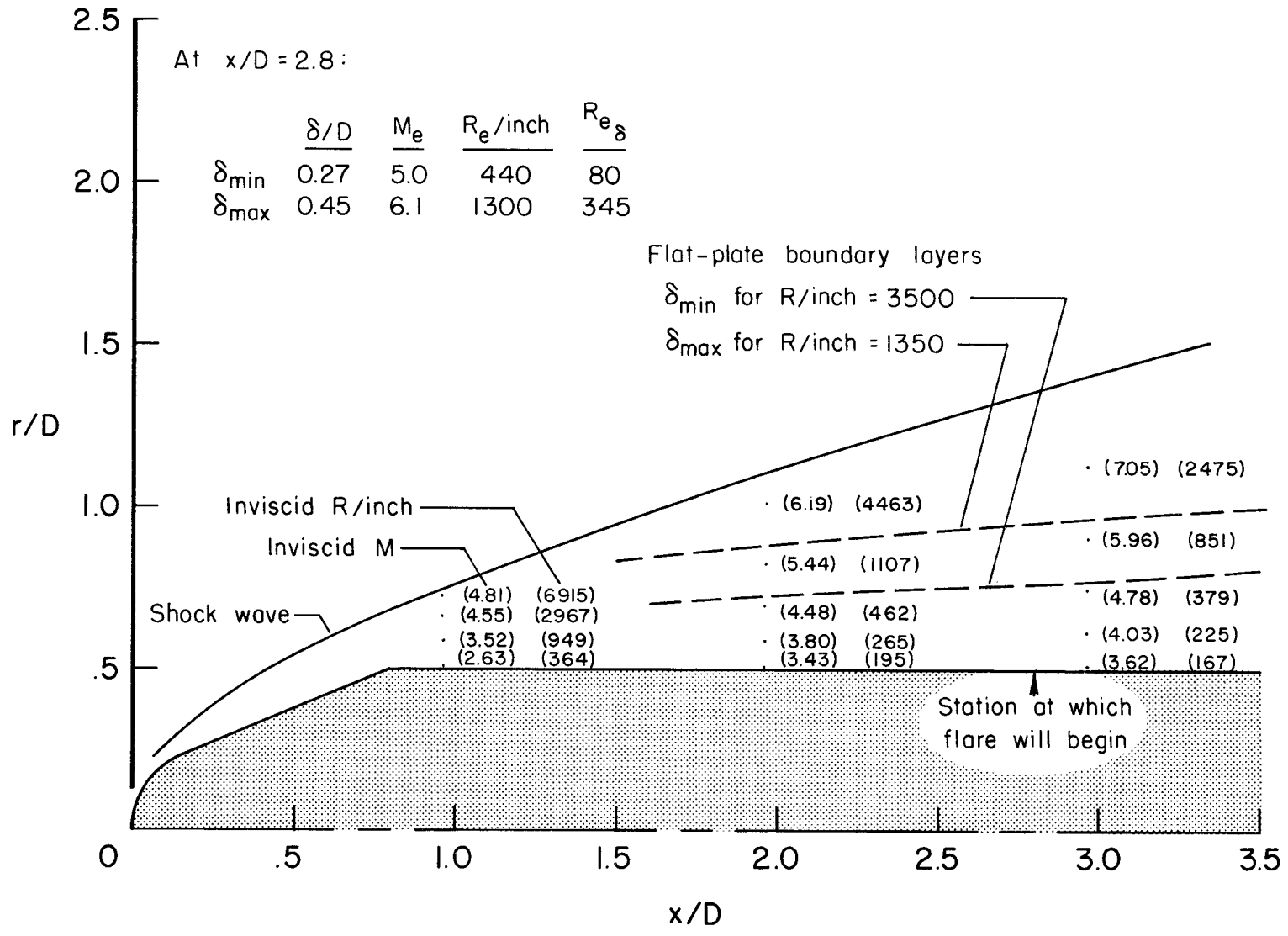

(a) Blunt conical-nosed cylinder.

Figure 3.- Estimated viscid-inviscid flow about the blunt cylinders; $M_{\infty_n} = 14.4$, $h_t = 1000$ Btu/lb, $R_{\infty_D} \sim 6200$.

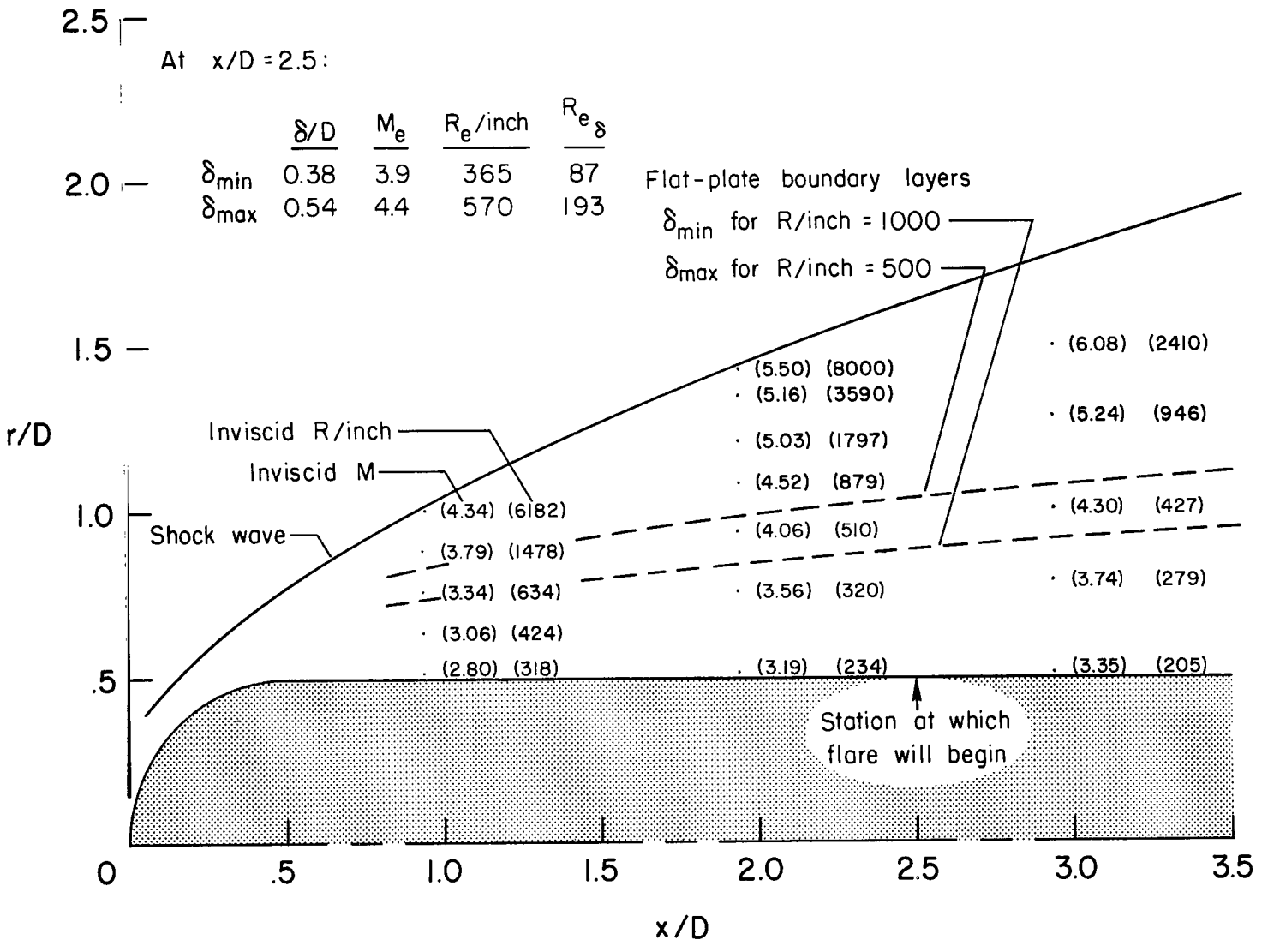

(b) Hemispherical-nosed cylinder.

Figure 3.- Continued.

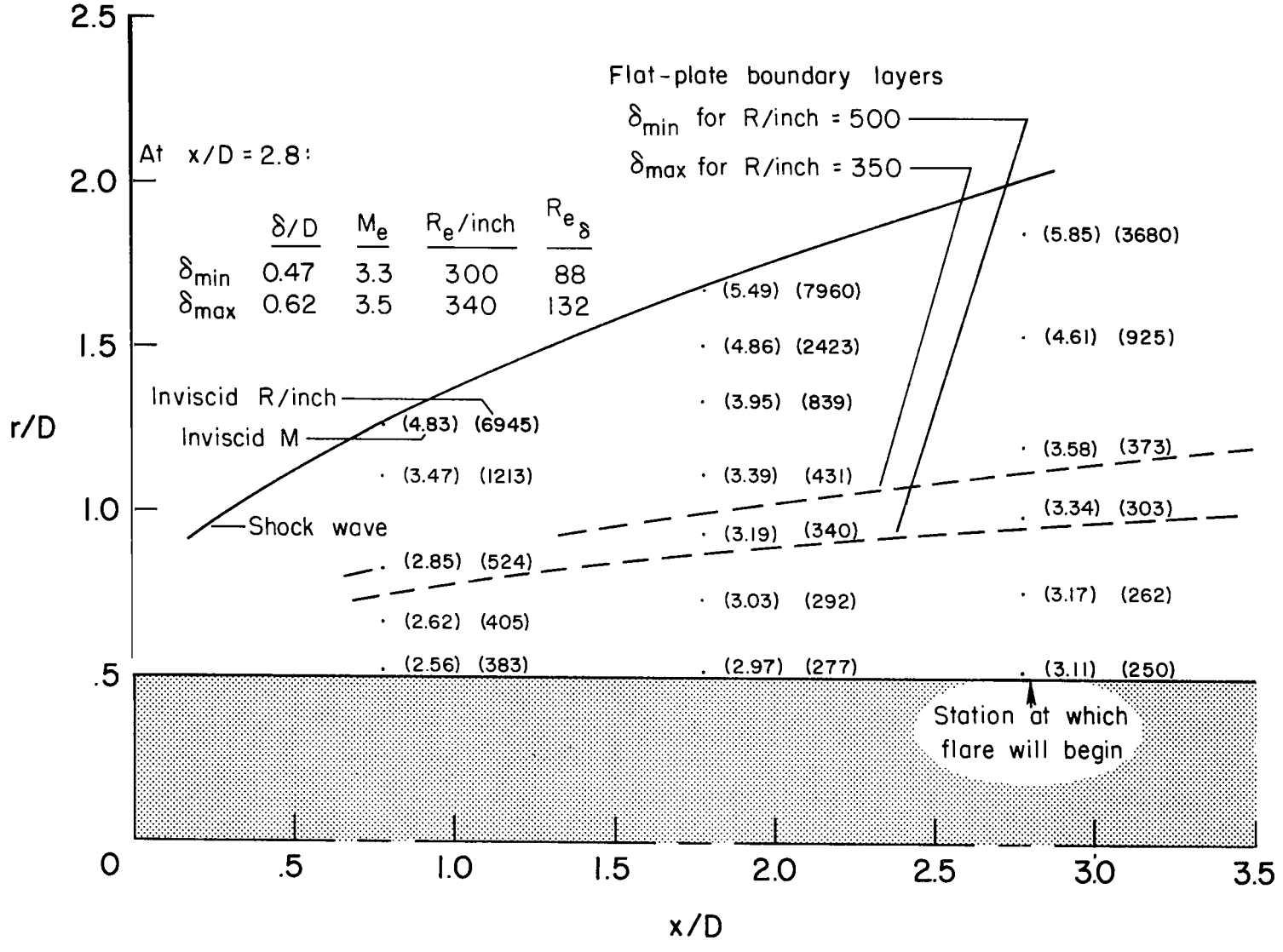

(c) Flat-nosed cylinder.

Figure 3.- Concluded.

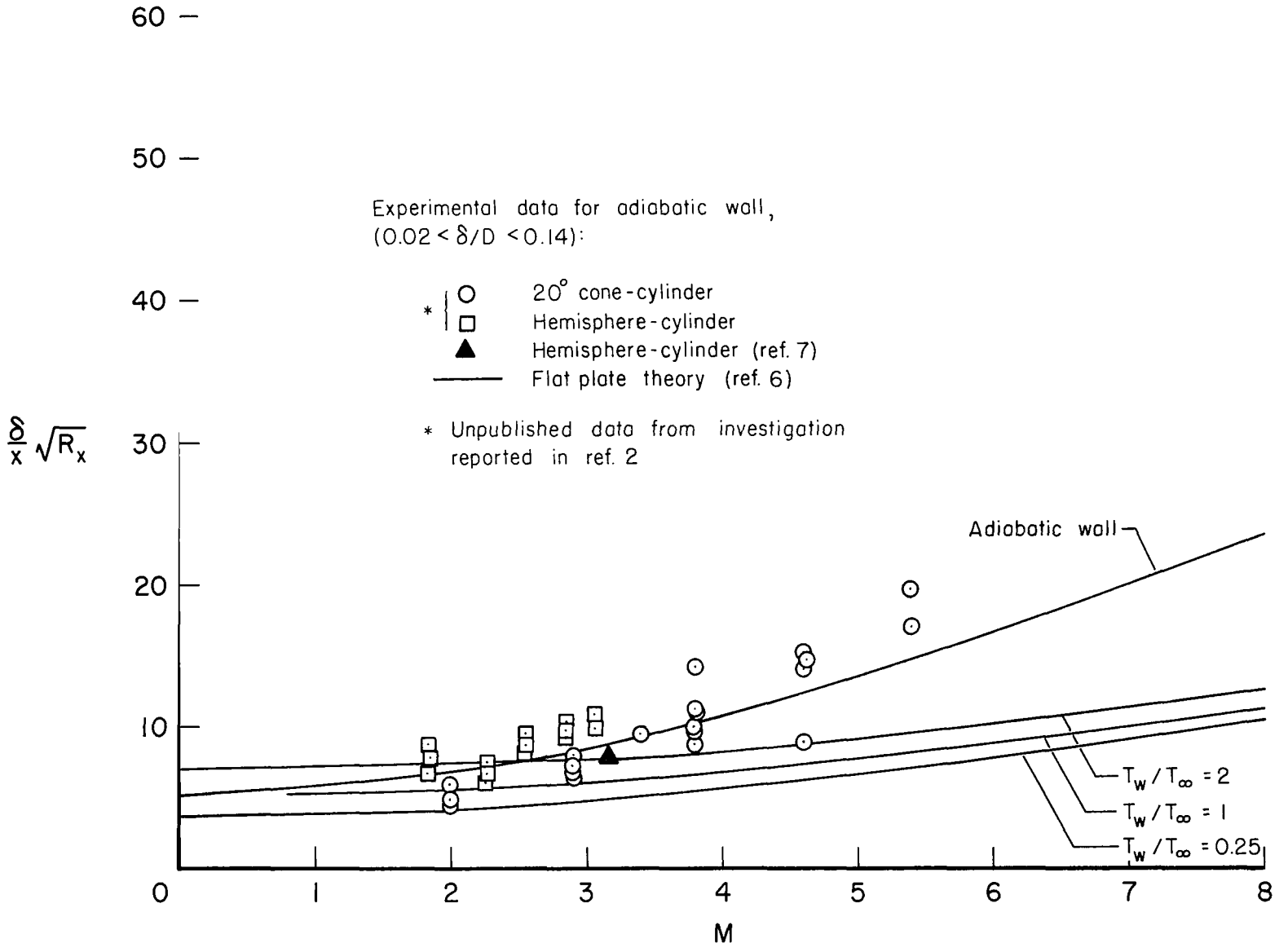

Figure 4.- Experimental values of boundary-layer thickness on axisymmetric bodies compared with flat-plate theory.

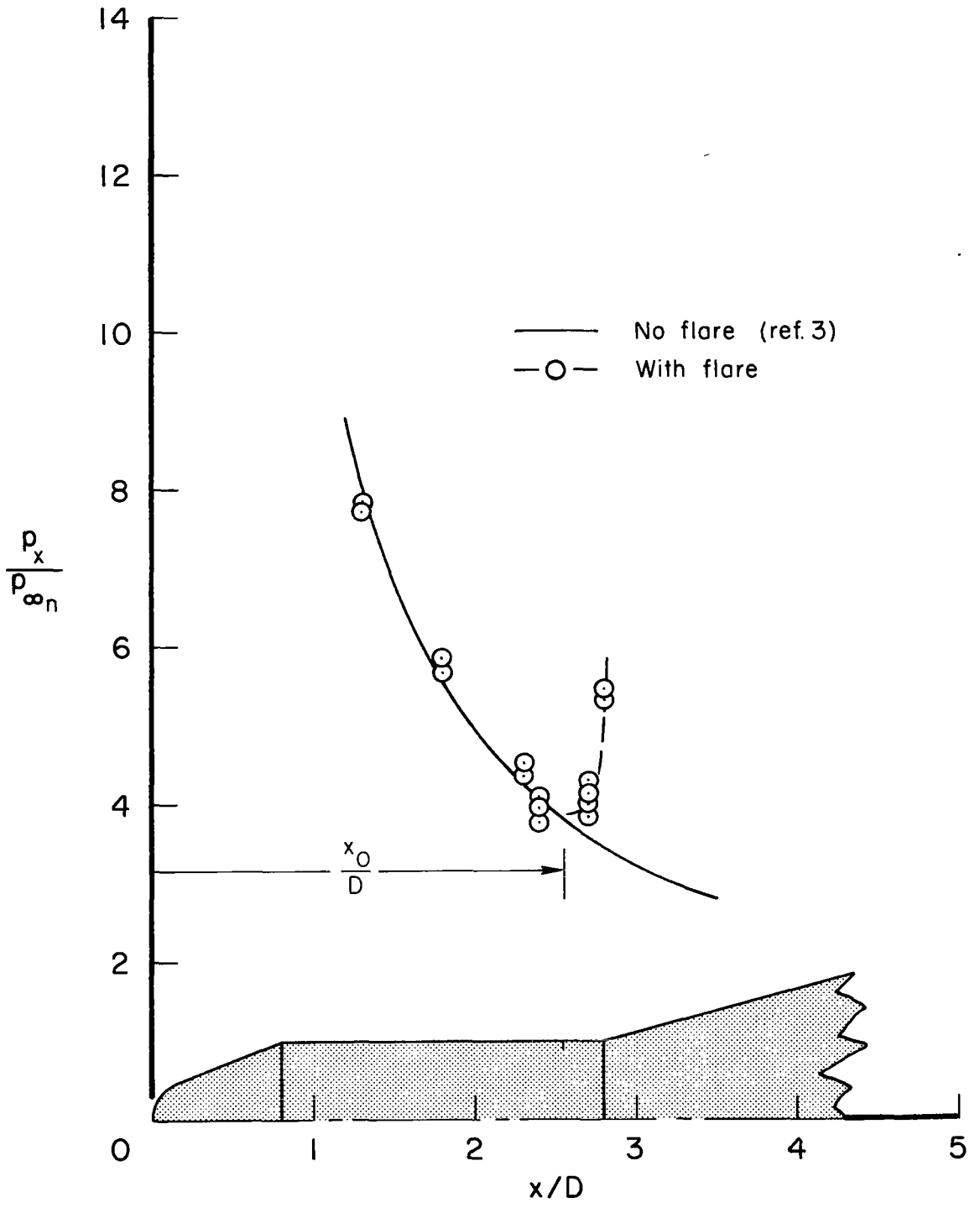

(a) $\theta = 15^{\circ}$, $p_{t_1} = 1000$ psia, $R_{\infty_D} \sim 6200$

Figure 5.- Surface pressure distributions on the blunt conical-nosed cylinder with and without a flare; $M_{\infty_n} = 14.4$, $h_t = 1000$ Btu/lb.

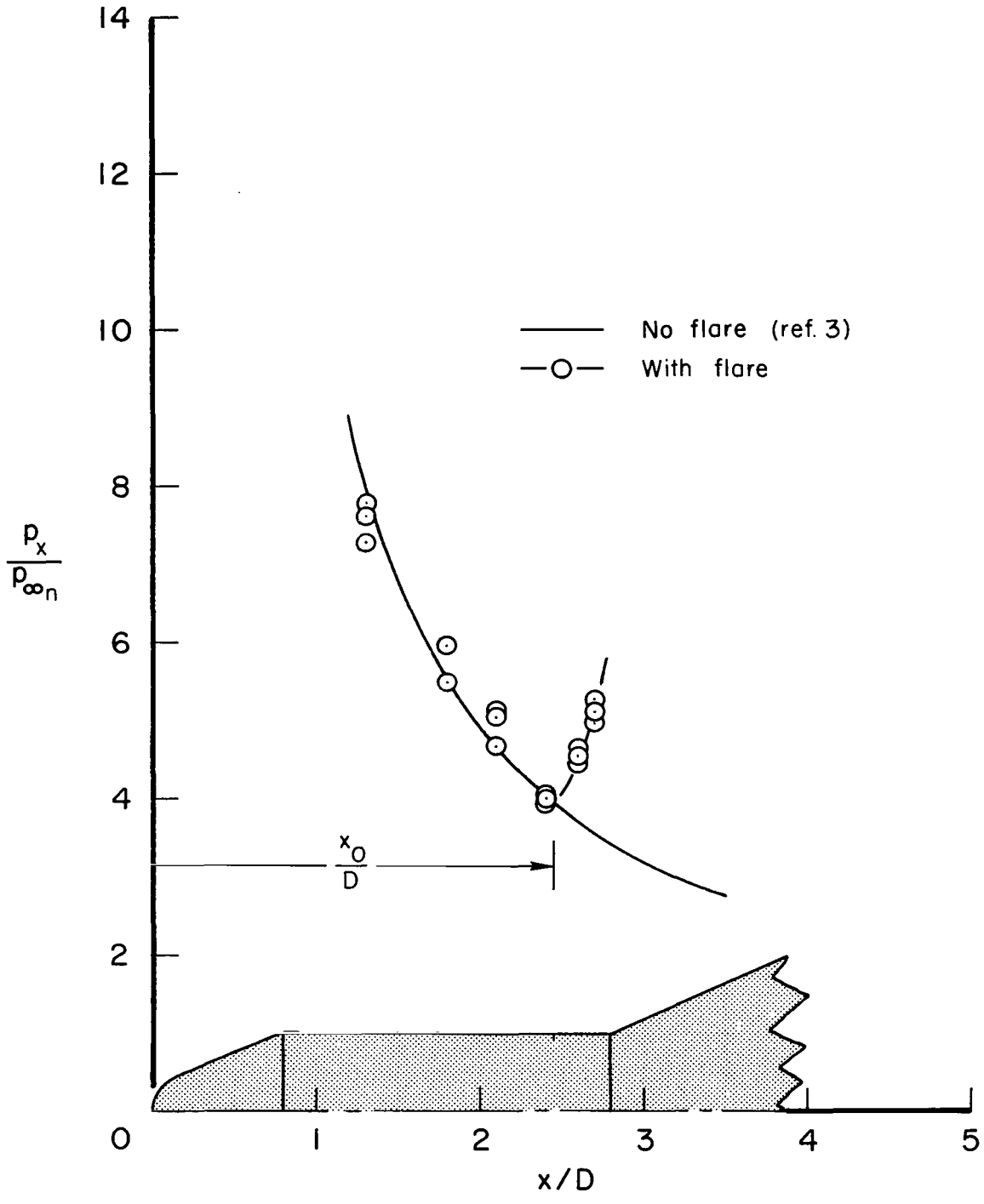

(b) $\theta = 25^{\circ}$, $p_{t_1} = 1000$ psia, $R_{\infty_D} \sim 6200$

Figure 5.- Continued

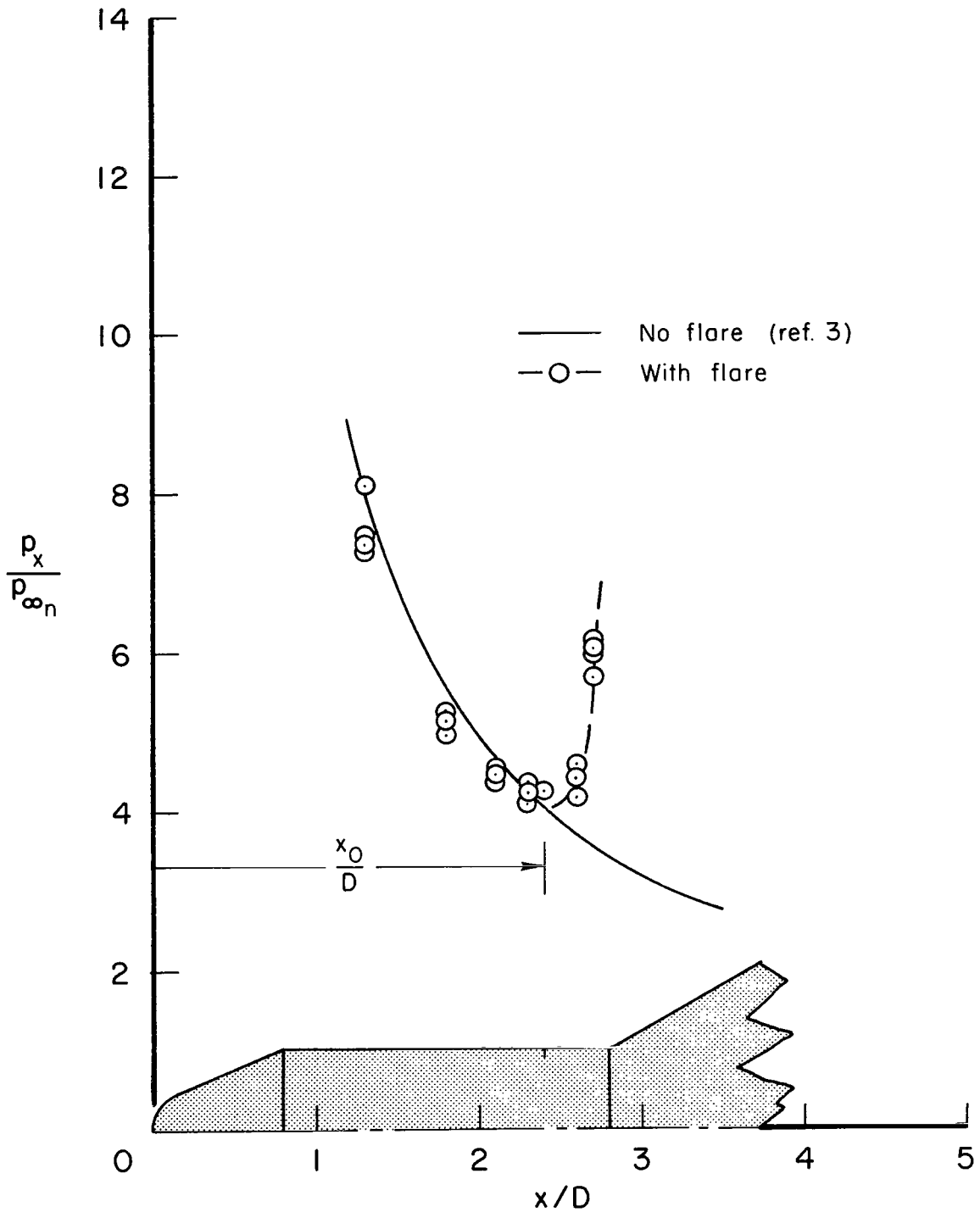

(c) $\theta = 30^{\circ}$, $p_{t_1} = 1000$ psia, R_{∞_D} ~6200

Figure 5.- Continued.

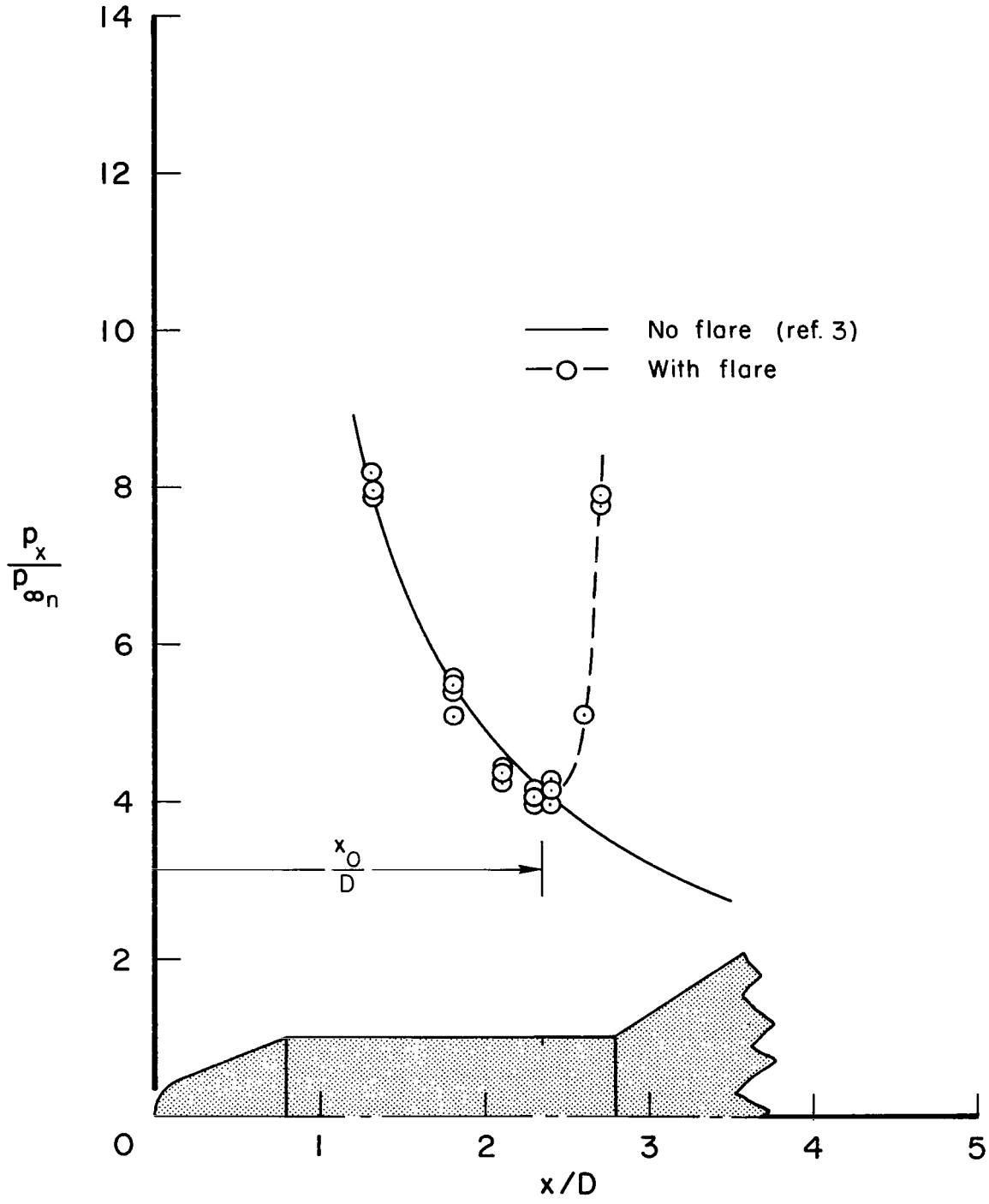

(d) $\theta = 35^{\circ}$, $p_{t_1} = 1000$ psia, $R_{\infty_D} \sim 6200$

Figure 5.- Continued.

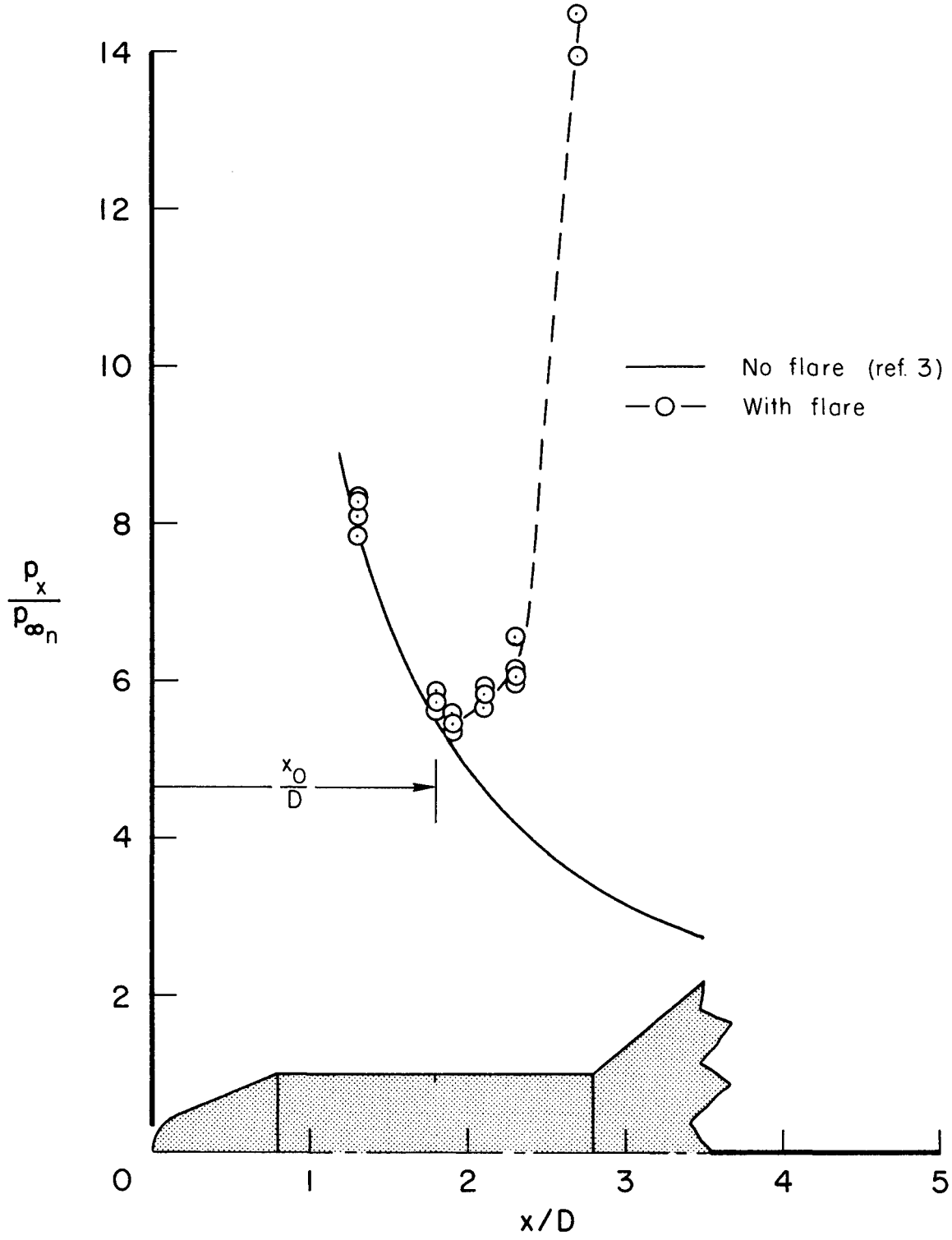

(e) $\theta = 40^{\circ}$, $p_{t_1} = 1000$ psia, R_{∞_D} ~6200

Figure 5.- Continued.

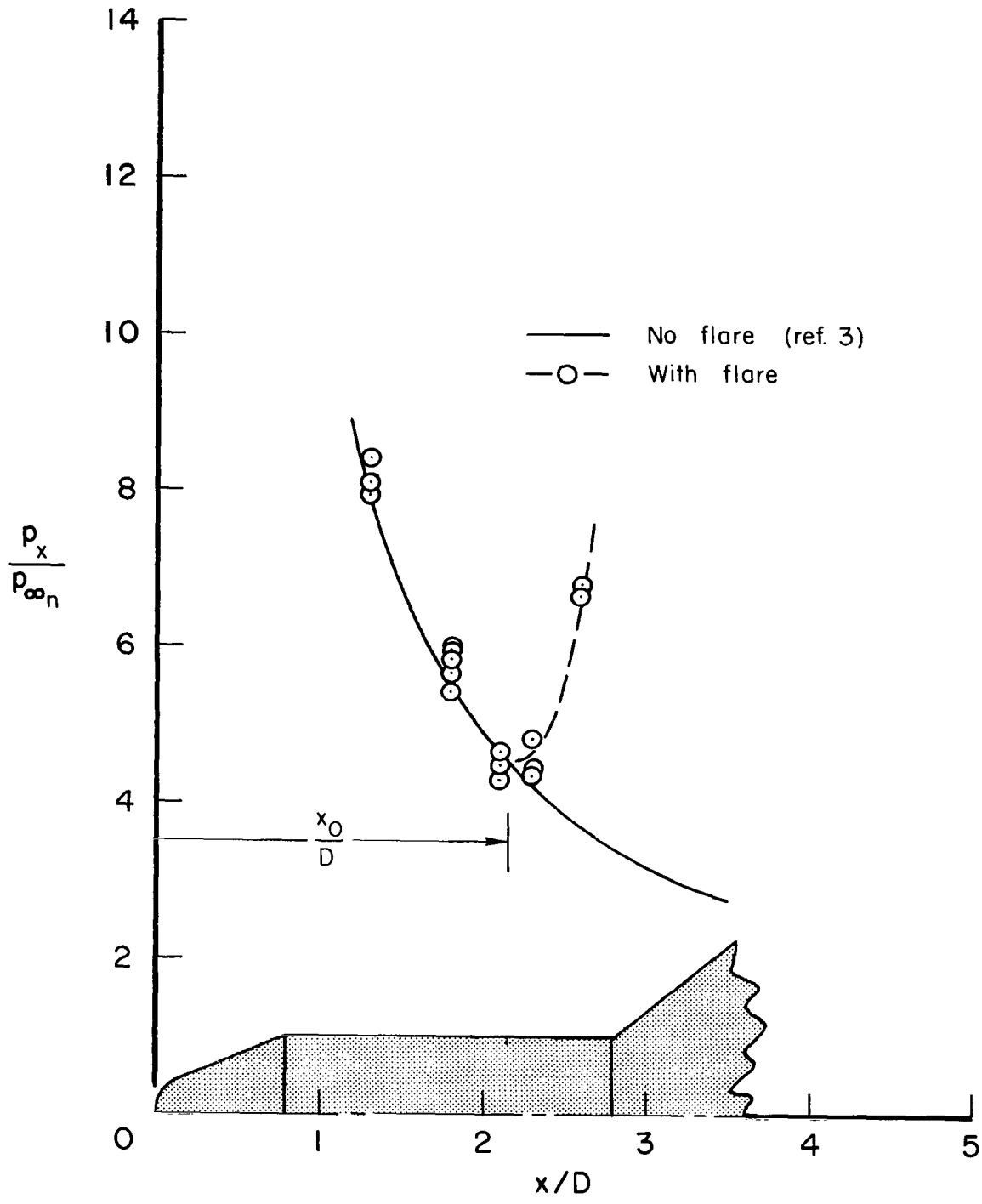

(f) $\theta = 40^\circ$, $p_{t_1} = 380$ psia, $R_{\infty_D} \sim 2400$

Figure 5.- Concluded.

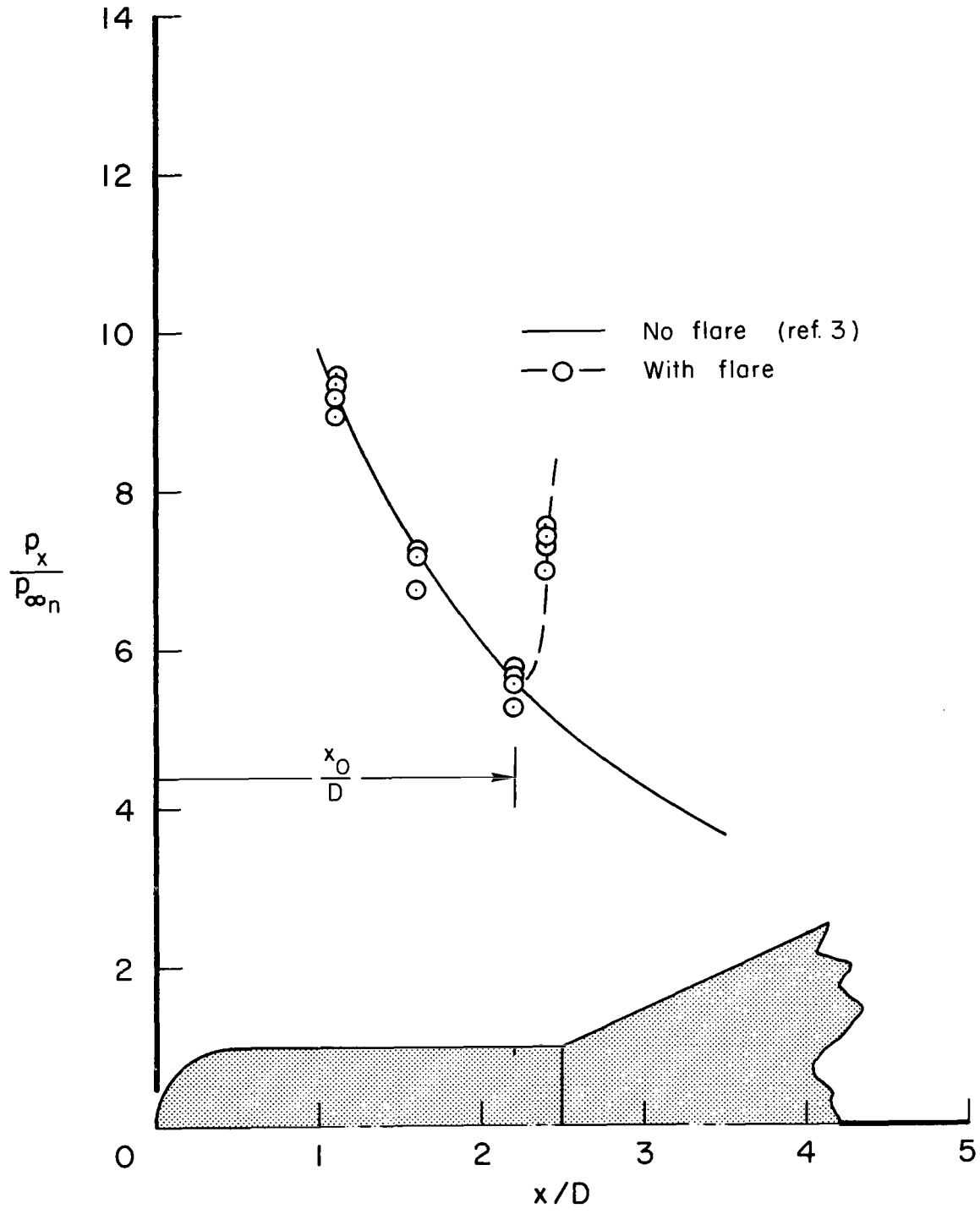

(a) $\theta = 25^{\circ}$, $p_{t_1} = 1000$ psia, $R_{\infty_D} \sim 6200$

Figure 6.- Surface pressure distributions on the hemispherical-nosed cylinder with and without flare; $M_{\infty_n} = 14.4$, $h_t = 1000$ btu/lb.

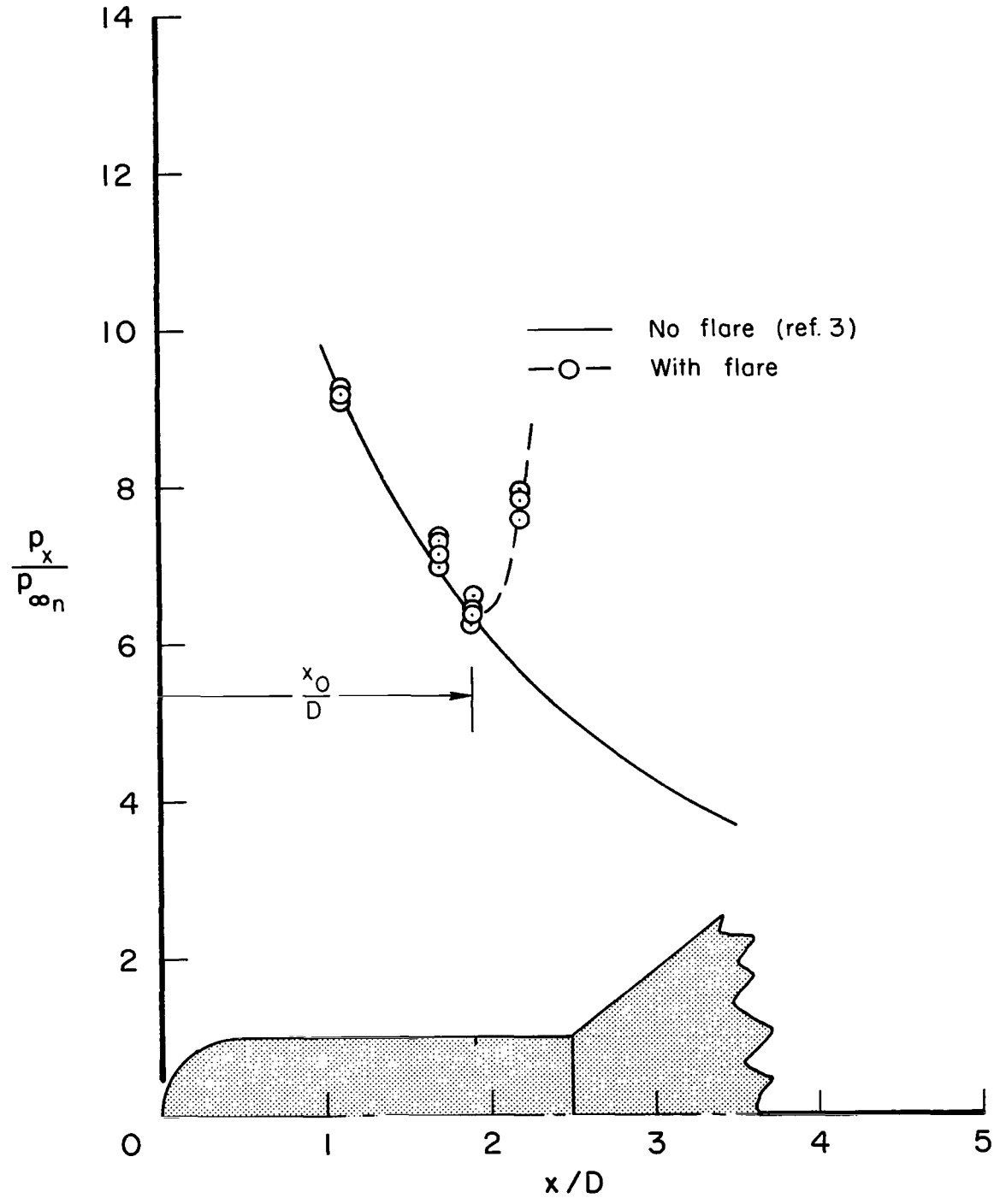

(b) $\theta = 40^{\circ}$, $p_{t_1} = 1000$ psia, $R_{\infty_D} \sim 6200$

Figure 6.- Concluded.

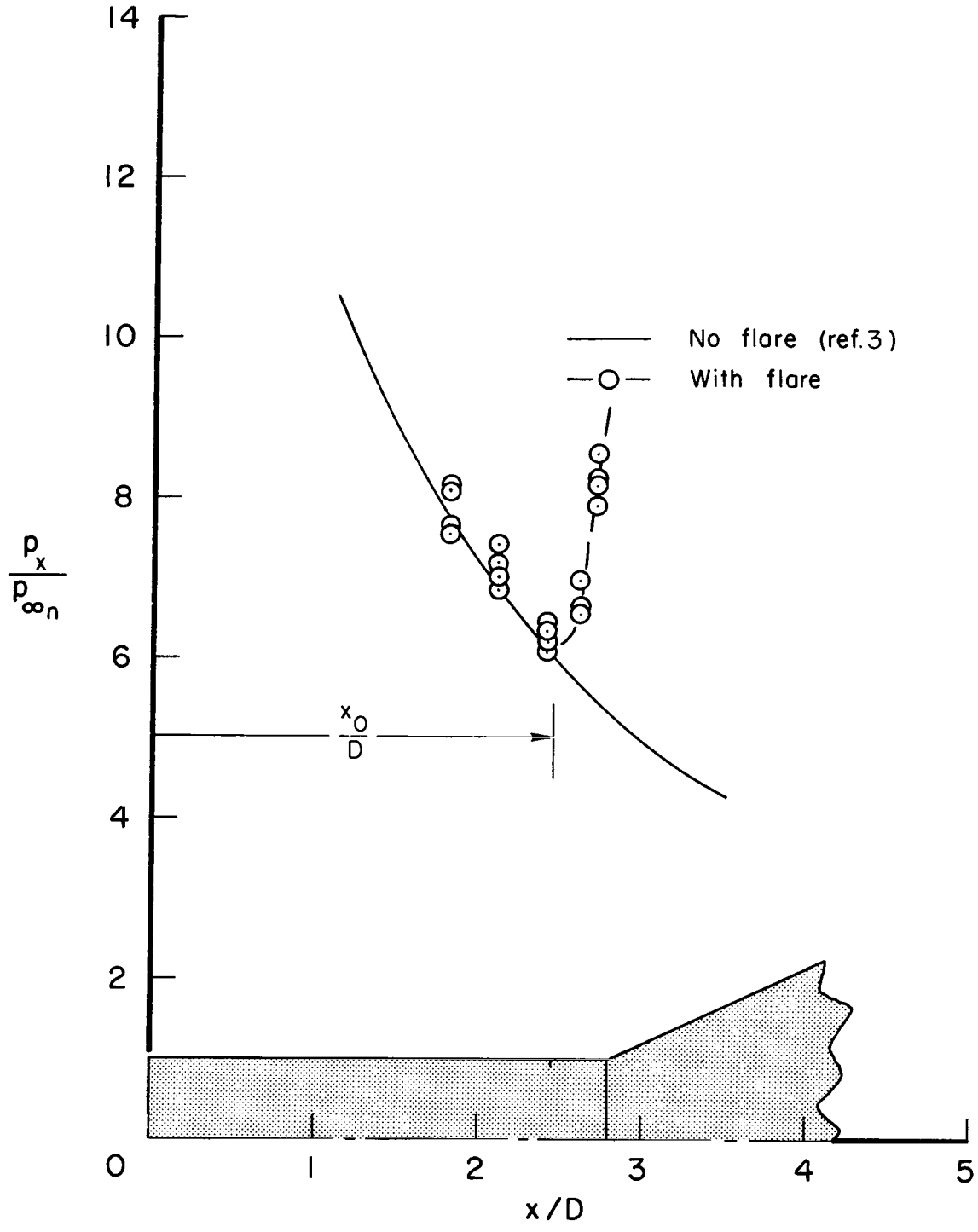

(a) $\theta = 25^{\circ}$, $p_{t_1} = 1000$ psia, $R_{\infty_D} \sim 6200$

Figure 7.- Surface pressure distributions on the flat-nosed cylinder with and without a flare; $M_{\infty_n} = 14.4$, $h_t = 1000$ Btu/lb.

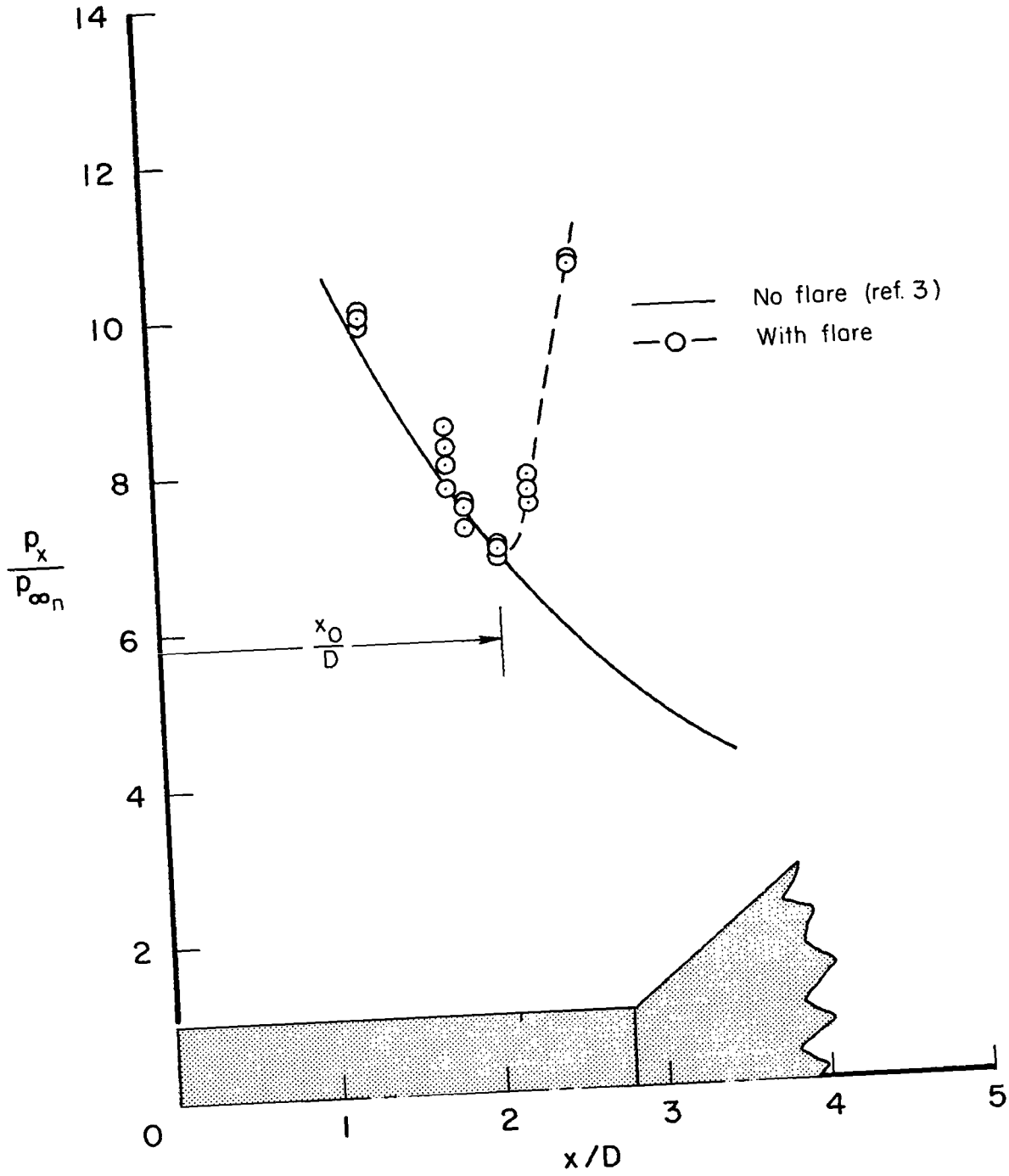

(b) $\theta = 40^{\circ}$, $p_{t_1} = 1000$ psia, $R_{\infty_D} \sim 6200$

Figure 7.- Concluded.

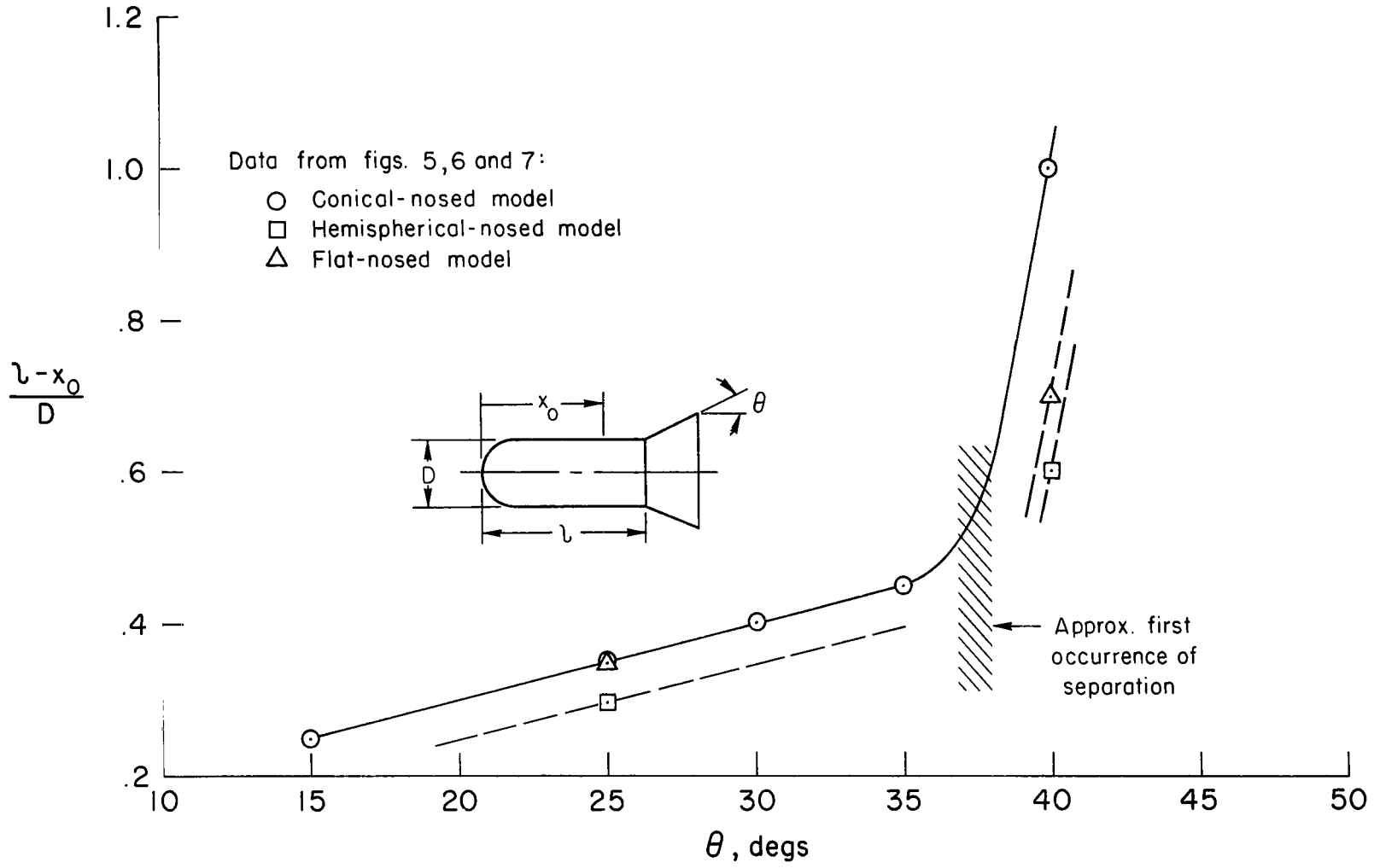

Figure 8.- Effect of flare angle on upstream infuence; M_{∞_n} = 14.4, h_t = 1000 Btu/lb, R_{∞_D} ~6200.

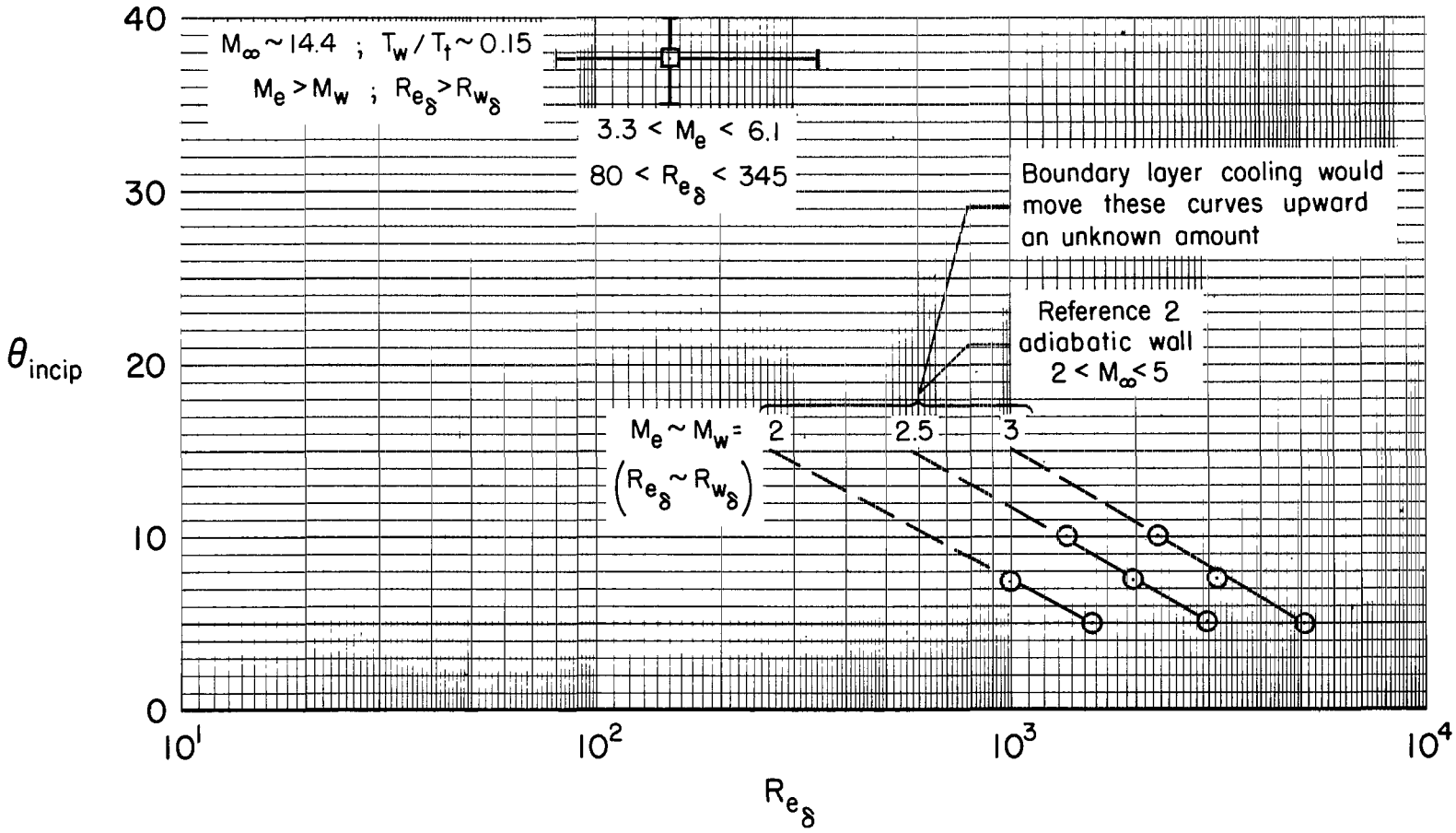

Figure 9.- Conditions for the incipient separation of a laminar boundary layer on a cylinder-flare configuration.

"The aeronautical and space activities of the United States shall be conducted so as to contribute . . . to the expansion of human knowledge of phenomena in the atmosphere and space. The Administration shall provide for the widest practicable and appropriate dissemination of information concerning its activities and the results thereof."

—NATIONAL AERONAUTICS AND SPACE ACT OF 1958

NASA SCIENTIFIC AND TECHNICAL PUBLICATIONS

TECHNICAL REPORTS: Scientific and technical information considered important, complete, and a lasting contribution to existing knowledge.

TECHNICAL NOTES: Information less broad in scope but nevertheless of importance as a contribution to existing knowledge.

TECHNICAL MEMORANDUMS: Information receiving limited distribution because of preliminary data, security classification, or other reasons.

CONTRACTOR REPORTS: Technical information generated in connection with a NASA contract or grant and released under NASA auspices.

TECHNICAL TRANSLATIONS: Information published in a foreign language considered to merit NASA distribution in English.

TECHNICAL REPRINTS: Information derived from NASA activities and initially published in the form of journal articles.

SPECIAL PUBLICATIONS: Information derived from or of value to NASA activities but not necessarily reporting the results of individual NASA-programmed scientific efforts. Publications include conference proceedings, monographs, data compilations, handbooks, sourcebooks, and special bibliographies.

Details on the availability of these publications may be obtained from:

SCIENTIFIC AND TECHNICAL INFORMATION DIVISION

NATIONAL AERONAUTICS AND SPACE ADMINISTRATION

Washington, D.C. 20546